This article is published as part of the *Dalton Transactions* themed issue entitled:

Radiopharmaceuticals for Imaging and Therapy

Guest Editors Stephen Faulkner (Oxford University) and Nick Long (Imperial College)

Published in issue 23, 2011 of *Dalton Transactions*

Image reproduced with permission of Martin W. Brechbiel

Articles in the issue include:

PERSPECTIVES:

ARTICLES:

Visit the *Dalton Transactions* website for more cutting-edge inorganic, organometallic and bioinorganic research
www.rsc.org/dalton

Dalton Transactions

Dynamic Article Links

Cite this: *Dalton Trans.*, 2011, **40**, 6268

www.rsc.org/dalton

PAPER

Dissociation kinetics of macrocyclic trivalent lanthanide complexes of 1,4,7,10-tetraazacyclododecane-1,7-diacetic acid (DO2A)†

Chih-Cheng Lin,[a,b] Chia-Ling Chen,[a] Kuan-Yu Liu[a,c] and C. Allen Chang*[a,c]

Received 21st October 2010, Accepted 12th January 2011
DOI: 10.1039/c0dt01440k

The $[H^+]$-catalyzed dissociation rate constants of several trivalent lanthanide (Ln) complexes of 1,4,7,10-tetraazacyclododecane-1,7-diacetic acid ($LnDO2A^+$, Ln = La, Pr, Eu, Er and Lu) have been determined in two pH ranges: 3.73–5.11 and 1.75–2.65 at four different temperatures (19–41.0 °C) in aqueous media at a constant ionic strength of 0.1 mol dm^{-3} ($LiClO_4$). For the study in the higher pH range, *i.e.* pH 3.73–5.11, copper(II) ion was used as the scavenger for the free ligand DO2A in acetate/acetic acid buffer medium. The rates of Ln(III) complex dissociation have been found to be independent of $[Cu^{2+}]$ and all the Ln(III) complexes studied show $[H^+]$-dependence at low acid concentrations but become $[H^+]$-independent at high acid concentrations. Influence of the acetate ion content in the buffer on the dissociation rate has also been investigated and all the complexes exhibit a first-order dependence on [Acetate]. The dissociation reactions follow the rate law: $k_{obs} = k_{Ac}[\text{Acetate}] + K'k_{lim}[H^+]/(1 + K'[H^+])$ where k_{AC} is the dissociation rate constant for the [Acetate]-dependent pathway, k_{lim} is the limiting rate constant, and K' is the equilibrium constant for the reaction $LnDO2A^+ + H^+ \Leftrightarrow LnDO2AH^{2+}$. In the lower pH range, *i.e.* pH 1.75–2.65, the dye indicator, cresol red, was used to monitor the dissociation rate, and all the Ln(III) complexes also show $[H^+]$-dependence dissociation pathways but without the rate saturation observed at higher pH range. The dissociation reactions follow the simple rate law: $k_{obs} = k_H[H^+]$, where k_H is the dissociation rate constant for the pathway involving monoprotonated species. The absence of an $[H^+]$-independent pathway in both pH ranges indicates that $LnDO2A^+$ complexes are kinetically rather inert. The obtained k_{AC} values follow the order: $LaDO2A^+ > PrDO2A^+ > EuDO2A^+ > ErDO2A^+ > LuDO2A^+$, whereas the k_{lim} and k_H values follow the order: $LaDO2A^+ > PrDO2A^+ > ErDO2A^+ > EuDO2A^+ > LuDO2A^+$, mostly consistent with their thermodynamic stability order, *i.e.* the more thermodynamically stable the more kinetically inert. In both pH ranges, activation parameters, ΔH^*, ΔS^* and ΔG^*, for both acetate-dependent and proton-catalyzed dissociation pathways have been obtained for most of the La(III), Pr(III), Eu(III), Er(III) and Lu(III) complexes, from the temperature dependence measurements of the rate constants in the 19–41 °C range. An isokinetic (linear) relationship is found between ΔH^* and ΔS^* values, which supports a common reaction mechanism.

Introduction

We have been interested in the basic understanding of the coordination chemistry such as thermodynamic,[1] kinetic,[2] structural,[3] and spectroscopic properties[4] as well as the design, synthesis and characterization of trivalent lanthanide (Ln) macrocyclic complexes for applications as magnetic resonance imaging contrast agents,[5] nuclear medicine,[6] luminescence probes,[7] solvent extraction agents,[8] and artificial nucleases.[9] Previously, we have reported the results of our studies on the formation stability, dissociation kinetics and structures of a number of Ln(III) complexes of macrocyclic ligands, including K21DA (dapda = 1,7-diaza-4,10,13-trioxacyclopentadecane-*N*,*N*′-diacetic acid[1b,c,2a]), K22DA (dacda = 1,10-diaza-4,7,13,16-tetraoxacyclooctadecane-*N*,*N*′-diacetic acid[1a,2b]), DO3A (1,4,7,10-tetraazacyclododecane-1,4,7-triacetic acid[2c,3a]), DOTA (1,4,7,10-tetraazacyclododecane-1,4,7,10-tetraacetic acid[2d,e]), and their structural analogs.[3a,4a,c,e] The cavity sizes, basicities, steric factors and conformations of the macrocyclic ligands all affect the physicochemical properties of their Ln(III) complexes, in particular, the formation stabilities and dissociation rates.[10]

[a]*Department of Biological Science and Technology, National Chiao Tung University, 75 Po-Ai Street, Hsinchu, Taiwan, 30039, R.O C*
[b]*Department of Cosmetics Application, Chin Min Institute of Technology, Taiwan*
[c]*Current address: Department of Biomedical Imaging and Radiological Sciences, National Yang-Ming University, No. 155, Sec. 2, Li-Nong St., Beitou, Taipei, Taiwan, 112, R.O.C. E-mail: cachang@ym.edu.tw; Fax: +886-2-28201093; Tel: +886-2-28201091*

† Electronic supplementary information (ESI) available: See DOI: 10.1039/c0dt01440k

Free lanthanide ions are not biologically essential and are toxic. With the use of gadolinium(III) complexes as magnetic resonance imaging (MRI) contrast agents as well as other potentially *in vivo*/*ex vivo* applications using trivalent lanthanide complexes such as luminescence probes for molecular imaging and artificial nucleases, it is important to understand the formation stabilities and dissociation kinetics of these lanthanide complexes. However, the majority of the studies on lanthanide complexes are focused on their thermodynamic, spectroscopic and structural aspects, fewer studies are on the kinetic aspects. It is our belief that high thermodynamic stability and low kinetic lability are preferred when trivalent lanthanide complexes are to be used as safe agents for medical and biological applications. For example, the European Medicines Agency has classified the gadolinium(III)-containing MRI contrast agents in three groups:[5i] (1) least likely (safest) to release free gadolinium ions Gd^{3+} in the body have a cyclical (macrocyclic) structure: Dotarem, Gadovist and ProHance; (2) intermediate have an ionic linear structure: Magnevist, MultiHance, Primovist (Eovist in the U.S.) and Vasovist; and (3) most likely to release Gd^{3+} have a linear non-ionic structure: Omniscan and OptiMARK. Among them, Omniscan, the gadolinium(III) complex of DTPA-BMA (diethylenetriamine-pentaacetic acid bis(methylamide)) causes the majority of cases of a rare and serious syndrome termed nephrogenic systemic fibrosis (NSF)[5j] and is probably related to its relatively low thermodynamic stability and high kinetic lability.

Lately, we have been designing macrocyclic Ln(III) complexes for use as artificial nucleases. A number of Ln(III) complexes of DO2A (1,4,7,10-tetraazacyclododecane-1,7-diacetic acid) as well as others have been studied to evaluate their efficiencies to catalyze phosphodiester bond hydrolysis of a model compound, BNPP (sodium bis(4-nitrophenyl)phosphate).[9] DO2A forms quite stable Ln(III) complexes and is kinetically rather inert. However, two different sets of $LnDO2A^+$ stability constants have been reported. The one reported by Sherry *et al.* used an out-of-cell potentiometric EDTA competition approach at pH 9–12 and the logarithmic stability constants are in the range 16.6–20.6 for La(III)–Yb(III) DO2A complexes.[11] The other set reported by us using capillary electrophoresis measurements of equilibrium concentrations of reaction species at lower pH indicated that the constants are smaller and are in the range 10.94–13.16 for the La(III)–Lu(III) DO2A complexes.[4f] The discrepancies remain to be explained and further studies, particularly complex dissociation kinetics, would be desirable because the complex formation stabilities are inversely related to their dissociation reaction rates.

In this paper we report the results of our study on the acid-catalyzed dissociation reaction kinetics of some Ln(III) complexes of DO2A. The structural formulae of ligands DO2A, K21DA and K22DA are shown in Scheme 1.

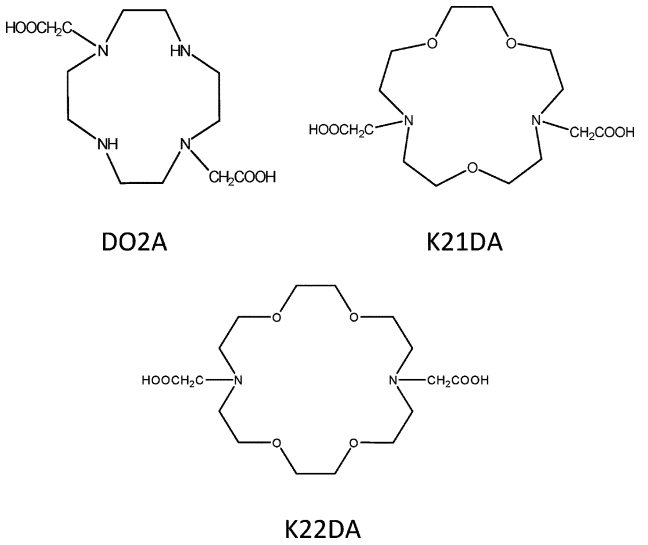

Scheme 1 Structural formulae of the ligands DO2A, K21DA and K22DA.

Results and discussion

$LnDO2A^+$ dissociation reactions in the pH range 3.73–5.11

DO2A forms relatively stable complexes with Ln(III) ions, although different stability constants were reported by different research groups.[4f,11] Calculations using the respective values of the protonation constants and the lower stability constants published previously indicate that ≥99% of Ln(III) ion exists in the complexed form at pH ≥ 6.5 under the conditions employed in this study.[4f] Because the stability of CuDO2A ($\log K_f = 18.9–21.99$)[12–14] is much greater than those of the corresponding Ln(III) complexes ($\log K_f$ = 10.94–13.16),[4f] the exchange reaction (eqn (1)) will be complete under the experimental conditions (20-fold excess of Cu^{2+}). This has been confirmed by reacting $LaDO2A^+$ (5.95×10^{-5} mol dm^{-3}) and $EuDO2A^+$ (5.0×10^{-5} mol dm^{-3}) separately with (1.0–5.0) mmol dm^{-3} Cu^{2+} salt solutions at pH 4.50, [Acetate] = 5.0 mmol dm^{-3}. The final average absorbance values were 0.222 ± 0.002 and 0.183 ± 0.002, respectively, which were in consistence with that if all DO2A ligand reacted with Cu^{2+} ions, *i.e.* 0.219 and 0.184, respectively ($\varepsilon_{CuDO2A,280\,nm} = 3680$). Thus, the experimental data fit pseudo-first-order kinetics with respect to the complex.

$$LnDO2A^+ + Cu^{2+} \rightarrow CuDO2A + Ln^{3+} \quad (1)$$

Independence of k_{obs} on $[Cu^{2+}]$. The k_{obs} values for the dissociation of the $LnDO2A^+$ (Ln = La, Eu, Lu) complexes show zero-order dependence on copper(II) ion concentration (Table S1, ESI†). Such a $[Cu^{2+}]$-independence in the dissociation kinetics of macrocyclic $LnK21DA^+$,[2a] and $LnK22DA^+$,[2b] complexes as well as other Ln(III) complexes[15–17] were also reported previously. Presumably, the copper(II) ion is unable to form a rate-determining, meta-stable binuclear intermediate with the $LnDO2A^+$ complex due to steric constraints imposed by the macrocycle when a Ln(III) ion is already present in its cavity. For the $LnDO2A^+$ complexes, the order of the dissociation rates is $LaDO2A^+ > EuDO2A^+ > LuDO2A^+$ which is consistent with the order of their formation stabilities, *i.e.* $\log K_f$ values 10.94, 12.99 and 13.16, respectively,[4f] and the greater the formation stability, the slower the dissociation rate.

It is noted that only in a few cases, $[Cu^{2+}]$-dependence were observed for the macrocyclic Ln(III) complex dissociation reactions, *e.g.* Ln(III) complexes of 1,4,10-triaza-7,13-dioxacyclopentadecane-*N*,*N*′,*N*″-tripropionic acid (N-pr_3[15]aneN_3O_2),[18] 1,7,13-triaza-4,10,16-trioxacyclooctadecane-*N*,*N*′,*N*″-triacetic acid (N-ac_3[18]aneN_3O_3),[19,20] and 1,7,13-triaza-4,10,16-trioxacyclooctadecane-*N*,*N*′,*N*″-trimethylacetic acid (N-ma_3[18]aneN_3O_3).[19,20] The first group of complexes has a 15-membered

Table 1 Effect of acetate concentration on $LnDO2A^+$ dissociation kinetics[a]

Ln(III)	La	Eu	Er	Lu
k_{AC}/mol^{-1}dm^{3}s^{-1}	$(1.12 \pm 0.05) \times 10^{-1}$	$(3.23 \pm 0.16) \times 10^{-3}$	$(8.62 \pm 1.31) \times 10^{-4}$	$(3.73 \pm 0.72) \times 10^{-4}$
k_0/s^{-1}	$(9.15 \pm 1.56) \times 10^{-5}$	$(3.99 \pm 0.53) \times 10^{-6}$	$(4.04 \pm 0.43) \times 10^{-6}$	$(1.38 \pm 0.23) \times 10^{-6}$
r^2	0.995	0.993	0.935	0.930
Ionic radius/Å	1.16	1.066	1.004	0.977

[a] pH = 4.61, [$LnDO2A^+$] = 5.0×10^{-5} mol dm^{-3}, [Acetate] = (1.0–5.0)$\times 10^{-3}$ mol dm^{-3}, [Cu^{2+}] = 1×10^{-3} mol dm^{-3}, T = 25 °C, μ = 0.1.

macrocyclic chelate ring and the stability constants of their Ln(III) complexes are: log K_f = 10.94–11.66. The latter two have 18-membered macrocyclic chelate rings and the log K_f value of the Gd(III)-N-ac$_3$[18]aneN$_3$O$_3$ complex is 18.02.[20] These three groups of Ln(III) complexes have relatively much faster dissociation reaction rates, which presumably may be related to either the less-stable and more flexible N-propionate chelate ring formation or the presence of several isomeric structures in aqueous solution[21,22] without the advantages of ligand pre-organization for metal ion complexation.[2e]

Acetate catalysis. Fig. 1 shows the plots of the k_{obs} values for the dissociation of selected $LnDO2A^+$ complexes against acetate ion concentrations and straight lines are obtained with appreciable slopes (full data are listed in Table S2, ESI†). Linear least squares regression analyses of the data give slope values k_{AC} (acetate-dependent rate constant) and intercept values k_0 (acetate-independent rate constant) with r^2 values close or equal to 1 (eqn (2), Table 1).

$$k_{obs} = k_0 + k_{AC}[\text{Acetate}] \quad (2)$$

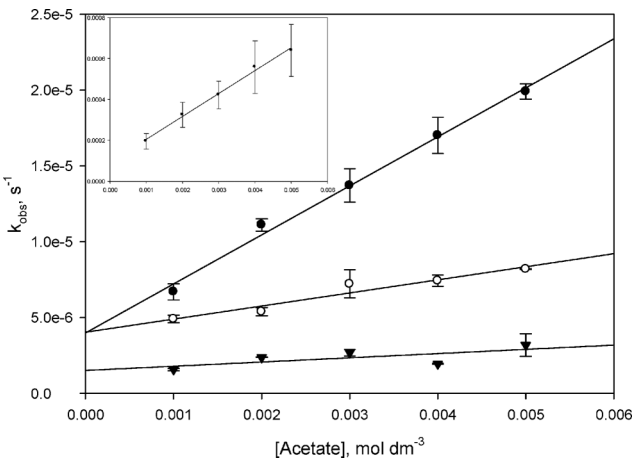

Fig. 1 Plots of dissociation k_{obs} (s^{-1}) values *vs.* [Acetate] (mol dm^{-3}) for selected $LnDO2A^+$ complexes; La (inset); Eu (●); Er (○); Lu (▼).

The enhanced rates of dissociation of these complexes in the presence of acetate ions can be attributed to the acetate ion complexation. The parent complexes are positively charged, and by the introduction of a negatively charged acetate ion into the coordination sphere they become neutral and labilized with respect to hydrogen ion attack. Under the experimental conditions, the observed k_{AC} value is the highest for $LaDO2A^+$ and it decreases with increasing atomic number of the Ln^{3+} ion. A plot of the log k_{Ac} values against the ionic radii of the Ln^{3+} ions is linear which may imply that the activation energy of the complex dissociation reaction is lowered more for the lighter lanthanide ions (plot not shown). This may also be related to the number of inner-sphere coordinated water molecules on the Ln^{3+} ion, *i.e.* the more the number of inner-sphere coordinated water molecules, the greater the chance for acetate ion to replace them, and the more lowered the activation energy. DO2A offers six coordination donor sites, the remaining inner-sphere coordination water molecules on the lanthanide ions are possibly four for $LaDO2A^+$, three for $EuDO2A^+$,[20] two to three for $ErDO2A^+$ and two for $LuDO2A^+$.[9a]

Among the four $LnDO2A^+$ complexes studied, the extent of acetate catalysis in complex dissociation is the greatest for $LaDO2A^+$. At [Acetate] = 5.0 mmol dm^{-3}, acetate catalysis constitutes an unprecedented 87% of the dissociation pathway of the $LaDO2A^+$ complex. Under the similar conditions, acetate catalysis constitutes only 21% of the dissociation pathway of $LaK21DA^+$ complex.[2a] The relative ease of acetate catalysis to enhance the dissociation rate of the $LaDO2A^+$ complex as compared to that of the $LaK21DA^+$ complex, may be related to a stronger acetate coordination to the $LaDO2A^+$ complex and the intrinsic slower dissociation rate of the $LaDO2A^+$ complex. Note that $EuK21DA^+$ has seven coordination donor atoms from the ligand and two inner-sphere coordinated water molecules.[4a] On the other hand, $EuK22DA^+$ with eight coordination donor atoms from the ligand and only one inner-sphere coordinated water molecule[4a] exhibits no anion-dependence for its dissociation reaction.[2b] The fact that k_0 is in the order $LaDO2A^+ > EuDO2A^+ \sim ErDO2A^+ > LuDO2A^+$, is roughly consistent with the trend of their formation constants (log $K_{f,\ ErDO2A^+}$ = 13.31)[4f] (*vide infra*).

Proton-independent and proton-dependent pathways. The k_{obs} values for the dissociation reactions (eqn (1)), the temperatures at which they were measured, and the concentrations of hydrogen ion are given in Table S3 (ESI†). When the observed rate constants are plotted against [H^+], saturation curves were obtained for all the Ln(III) complexes studied, *i.e.* the observed rate constants show [H^+]-dependence at low acid concentrations but become [H^+]-independent at high acid concentrations (Fig. 2). All plots show appreciable intercepts that correspond to the proton-independent dissociation rate constants. The proposed mechanisms are shown in Scheme 2 where Ln, L, LnL and LnHL are the Ln(III) ion, ligand (DO2A), Ln(III) complex and protonated Ln(III) complex, respectively.

The rate law consistent with the proposed mechanisms is:

$$k_{obs} = k_d + k_{AC}[\text{Acetate}] + K'k_{lim}[H^+]/(1 + K'[H^+]) \quad (3)$$

I: Proton-independent direct dissociation pathway

$$LnL^{+} \underset{k_{-d}}{\overset{k_d}{\rightleftarrows}} [LnL^{+}]^{*} \xrightarrow[\text{fast}]{Cu^{2+}/H^{+}} Ln^{3+} + CuL + H^{+}$$

II: Acetate-dependent dissociation pathway

$$LnL^{+} + Ac^{-} \underset{k_{AC}}{\overset{k_{AC}}{\rightleftarrows}} [LnL(Ac)] \xrightarrow[\text{fast}]{Cu^{2+}} Ln^{3+} + CuL + Ac^{-}$$

III: Proton-dependent, limiting rate dissociation pathway

$$LnL^{+} + H^{+} \underset{k_{-H}}{\overset{k_H}{\rightleftarrows}} [LnLH^{2+}] \xrightarrow{k_{lim}} [LnLH^{2+}]^{*} \xrightarrow[\text{fast}]{Cu^{2+}} Ln^{3+} + CuL + H^{+}$$

Scheme 2 The proposed mechanisms for the dissociation of $LnDO2A^{+}$ in the pH range 3.73–5.11.

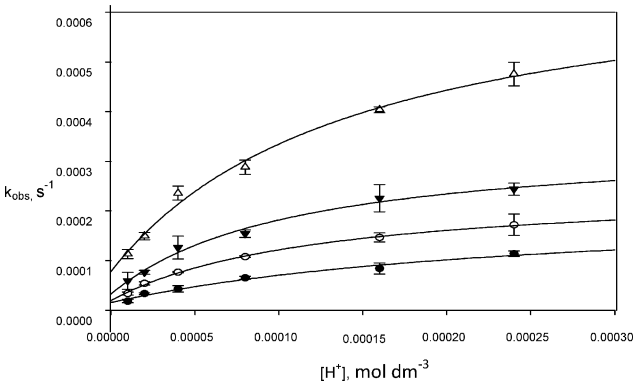

Fig. 2 Plots of the dissociation k_{obs} values *vs.* $[H^{+}]$ for the $PrDO2A^{+}$ complex at different temperatures: 19 °C (●); 25 °C (○); 33 °C (▼); 41 °C (△).

where k_d is the proton-independent direct dissociation rate constant, K' ($= k_H/k_H'$) is the equilibrium constant for the formation of the monoprotonated complex (eqn (4)), and k_{lim} is the limiting rate constant for the protonated lanthanide complex.

$$LnL^{+} + H^{+} = LnLH^{2+} \quad (4)$$

Note that k_0 in eqn (2) is equal to $k_d + K'k_{lim}[H^{+}]/(1 + K'[H^{+}])$ in eqn (3). Because [Acetate] = 5.0 mmol dm^{-3}, the term $k_d + k_{AC}$[Acetate] should not vary with $[H^{+}]$ and eqn (3) can be written as

$$k_{obs} = k_d' + K'k_{lim}[H^{+}]/(1 + K'[H^{+}]) \quad (5)$$

where $k_d' = k_d + k_{AC}$[Acetate]. The values of k_d', k_{lim} and K' are resolved by an unweighted least-squares analysis and are listed in Table 2.

It is further noted that if the k_{AC} values obtained in Table 1 at 25 °C are used to calculate the k_{AC}[Acetate] values and are subtracted from the corresponding k_d' values, the resulted k_d values are all negative. This indicates that the direct dissociation pathway is negligible in the present system and the rate law can be simplified as

$$k_{obs} = k_{AC}[Acetate] + K'k_{lim}[H^{+}]/(1 + K'[H^{+}]) \quad (6)$$

and $k_d' \simeq k_{AC}$[Acetate]. Thus, the k_{AC} values for various LnL complexes at different temperatures could be calculated by k_d'/[Acetate] using the data in Table 2, where [Acetate] = 0.005 mol dm^{-3}.

The regular decrease in k_d' (*i.e.* k_{AC}) values of the $LnDO2A^{+}$ complexes from La(III) to Er(III) have been discussed previously (*vide supra*) which happens to be the same trend of their thermodynamic stabilities. On the other hand, the limiting rate constants (k_{lim}) are in a slightly different order La > Pr > Er > Eu. The fact that all the log K' values are in the 2–3 range which are similar to those found for the heavy lanthanide (Tb^{3+}–Lu^{3+}) complexes of K21DA, also reflects similarities of the dissociation mechanisms of the $LnDO2A^{+}$ and the heavy $LnK21DA^{+}$ (Ln = Tb^{3+}–Lu^{3+}) complexes.

The k_{lim} values for the $LnDO2A^{+}$ complexes are about two to three orders of magnitude smaller than the corresponding ones of the heavy $LnK21DA^{+}$ complexes, indicating that the ligand DO2A with a smaller macrocyclic ring size tends to form more rigid Ln(III) complexes which dissociate more slowly than those of the larger-sized and more flexible ligand, $LnK21DA^{+}$. Indeed,

Table 2 Resolved rate and equilibrium constants for the dissociation reactions of $LnDO2A^{+}$ complexes at various temperatures

Ln^{3+}	T/°C	k_d'/s^{-1}	k_{lim}/s^{-1}	K'/mol^{-1} dm^3	r^2
La	19	$(1.88 \pm 0.59) \times 10^{-4}$	$(1.80 \pm 0.60) \times 10^{-3}$	$(3.86 \pm 2.56) \times 10^{+3}$	0.983
	25	$(3.09 \pm 0.79) \times 10^{-4}$	$(2.70 \pm 0.53) \times 10^{-3}$	$(4.91 \pm 2.20) \times 10^{+3}$	0.991
	33	$(3.82 \pm 1.56) \times 10^{-4}$	$(3.82 \pm 0.45) \times 10^{-3}$	$(8.02 \pm 3.06) \times 10^{+3}$	0.990
	41	$(6.86 \pm 1.33) \times 10^{-4}$	$(6.00 \pm 0.27) \times 10^{-3}$	$(9.52 \pm 1.70) \times 10^{+3}$	0.998
Pr	19	$(1.55 \pm 0.65) \times 10^{-5}$	$(1.97 \pm 0.64) \times 10^{-4}$	$(3.90 \pm 2.57) \times 10^{+3}$	0.984
	25	$(1.94 \pm 0.40) \times 10^{-5}$	$(2.29 \pm 0.11) \times 10^{-4}$	$(8.06 \pm 1.30) \times 10^{+3}$	0.992
	33	$(3.24 \pm 1.43) \times 10^{-5}$	$(3.11 \pm 0.32) \times 10^{-4}$	$(9.24 \pm 3.49) \times 10^{+3}$	0.990
	41	$(7.79 \pm 2.04) \times 10^{-5}$	$(6.32 \pm 0.77) \times 10^{-4}$	$(6.84 \pm 2.40) \times 10^{+3}$	0.993
Eu	19	$(2.20 \pm 1.89) \times 10^{-6}$	$(5.71 \pm 1.47) \times 10^{-5}$	$(4.49 \pm 2.51) \times 10^{+3}$	0.986
	25	$(7.86 \pm 2.63) \times 10^{-6}$	$(1.14 \pm 0.15) \times 10^{-4}$	$(5.46 \pm 1.73) \times 10^{+3}$	0.995
	33	$(1.15 \pm 0.60) \times 10^{-5}$	$(1.98 \pm 0.51) \times 10^{-4}$	$(4.28 \pm 2.31) \times 10^{+3}$	0.988
	41	$(2.03 \pm 1.12) \times 10^{-5}$	$(3.56 \pm 0.75) \times 10^{-4}$	$(4.89 \pm 2.36) \times 10^{+3}$	0.989
Er	19	$(1.07 \pm 0.41) \times 10^{-6}$	$(9.24 \pm 1.22) \times 10^{-5}$	$(2.09 \pm 0.42) \times 10^{+3}$	0.999
	25	$(3.03 \pm 0.92) \times 10^{-6}$	$(1.80 \pm 0.44) \times 10^{-4}$	$(1.58 \pm 0.55) \times 10^{+3}$	0.998
	33	$(3.93 \pm 0.94) \times 10^{-6}$	$(2.09 \pm 0.12) \times 10^{-4}$	$(3.33 \pm 0.36) \times 10^{+3}$	1.000
	41	$(8.54 \pm 12.5) \times 10^{-6}$	$(5.38 \pm 1.63) \times 10^{-4}$	$(3.34 \pm 1.88) \times 10^{+3}$	0.990
Lu	25	$(4.99 \pm 1.34) \times 10^{-7}$	$(3.20 \pm 0.33) \times 10^{-5}$	$(2.31 \pm 0.38) \times 10^{+3}$	0.999

Table 3 Molar activation parameters for acetate-dependent dissociation and proton-dependent dissociation of selected $LnDO2A^+$, $LnK21DA^+$ and $LnK22DA^+$ complexes. ΔG^* values are calculated at 25 °C

LnL	ΔH_{AC}*/kcal	ΔS_{AC}*/cal K^{-1}	ΔG_{AC}*/kcal	ΔH_{lim}*/kcal	ΔS_{lim}*/cal K^{-1}	ΔG_{lim}*/kcal
$LaDO2A^+$	9.4 ± 1.4	−32.6 ± 7.0	19.1	9.1 ± 0.5	−39.9 ± 2.3	21.0
$PrDO2A^+$	12.7 ± 2.2	−26.8 ± 9.9	20.0	8.8 ± 2.0	−45.5 ± 10.9	22.4
$EuDO2A^+$	16.5 ± 3.9	−16.9 ± 12.9	21.1	14.2 ± 1.0	−29.2 ± 3.6	22.9
$ErDO2A^+$	15.2 ± 3.0	−22.9 ± 11.9	22.0	12.7 ± 2.7	−33.4 ± 10.6	22.7
	ΔH_d*/kcal	ΔS_d*/cal K^{-1}	ΔG_d*/kcal	ΔH_{lim}*/kcal	ΔS_{lim}*/cal K^{-1}	ΔG_{lim}*/kcal
$LaK21DA^+$	4.7	−49.5	19.5	n/a		
$EuK21DA^+$	6.9	−48.6	21.4	n/a		
$ErK21DA^+$	7.9	−43.4	20.8	14.0	−20.8	20.2
$LuK21DA^+$	8.0	−40.5	20.1	15.6	−12.6	19.4
$EuK22DA^+$	7.9 ± 1.7	−47.5 ± 9.4	22.1	n/a		

the k_{obs} values of the LnL^+ complexes (L = K21DA and DO2A) obtained in similar pH ranges are in the order $LnK21DA^+ > LnDO2A^+$.

Activation parameters. The activation parameters for the proton-independent and proton-dependent pathways have been obtained from the temperature dependence measurements of rate constants. According to the Eyring equation (7),[23]

$$\ln(k/T) = \ln(k_B/h) - (\Delta H^*/RT) + (\Delta S^*/R) \quad (7)$$

the activation parameters of these dissociation reactions can be obtained by plotting of $\ln(k/T)$ *vs.* $1/T$, where k is the rate constant, R is gas constant (1.987 cal mol^{-1} K^{-1}—this unit is used for convenient comparisons with previously published data), k_B is Boltzmann's constant (1.381×10^{-23} J K^{-1}), h is Planck's constant (6.626×10^{-34} J s) and T is absolute temperature (Fig. 3). The slope and intercept values of these plots yield the activation enthalpy (ΔH^*) and entropy (ΔS^*) data:

$$\text{slope} = (-\Delta H^*/R) \quad (8)$$

$$\text{intercept} = (\Delta S^*/R) + \ln(k_B/h) \quad (9)$$

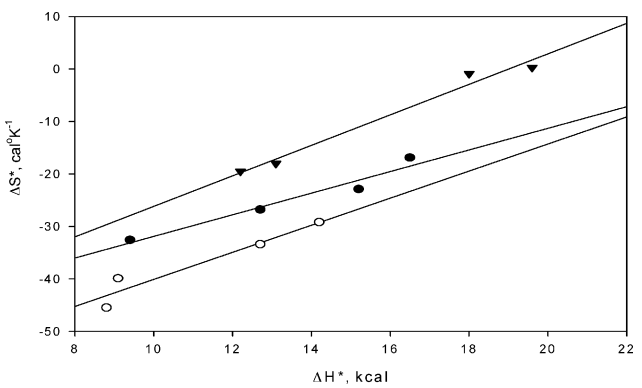

Fig. 3 Plots of values of ΔH^* *vs.* ΔS^*. Data are from Table 3: (●) k_{AC} pathway, pH range 3.73–5.11; (○) k_{lim} pathway, pH range 3.73–5.11; (▼) k_H pathway, pH range 1.75–2.65 (*vide infra*).

The free energy of activation, ΔG^*, can be calculated according to the following equation:

$$\Delta G^* = \Delta H^* - T\Delta S^* \quad (10)$$

Table 3 lists the values of ΔH^*, ΔS^* and ΔG^* (25 °C) obtained from the Eyring plots for the acetate-dependent and proton-dependent dissociation reaction pathways of $LnDO2A^+$ (plots not shown). For comparison purposes, the data for selected $LnK21DA^+$ complexes are also included in Table 3. An interesting isokinetic (linear) relationship is observed when the values of ΔH^* are plotted against those of ΔS^* (Fig. 3).[24a,25] This indicates that the dissociation of all the $LnDO2A^+$ complexes studied follow a similar dissociation mechanism.

The $EuDO2A^+$ complex has the greatest temperature variations on both k_{AC} and k_{lim} values leading to the highest ΔH_{AC}^* and ΔH_{lim}^* values among all $LnDO2A^+$ complexes studied. On the other hand, due to its less unfavorable ΔS^* barrier, the trend for the overall ΔG^* values is still $LaDO2A^+ < PrDO2A^+ < EuDO2A^+ \leq ErDO2A^+$, for both the acetate-dependent and proton-dependent pathways, which is in the same order as their formation stabilities. (Note that the ΔG_{lim}^* values for the respective $EuDO2A^+$ and $ErDO2A^+$ complexes are 22.9 and 22.7 kcal mol^{-1}, which might be considered similar within the experimental error limits.)

The ΔH_{AC}^* values of $LnDO2A^+$ complexes are all greater than those of the ΔH_d^* values of the corresponding $LnK21DA^+$ complexes. On the other hand, the ΔS_{AC}^* values of $LnDO2A^+$ are all less negative than those of the ΔS_d^* values of the corresponding $LnK21DA^+$ complexes. These observations might be related to the fact that DO2A is more rigid than K21DA and that the acetate-dependent dissociation pathway involves charge neutralization when the LnDO2A(Ac) ternary complex is formed,[24b] respectively. The ΔG_{AC}^* values are all smaller than the corresponding ΔG_{lim}^* values at 25 °C, indicating that the acetate-dependent dissociation pathways are quite competitive as compared to the proton-dependent, limiting rate ones owing to less negative ΔS^* values.

The ΔG_{lim}^* values at 25 °C for the proton-dependent pathways are all greater than those of the $LnK21DA^+$ complexes,[2a] reflecting the higher thermodynamic stability of the $LnDO2A^+$ complexes. Comparing the ΔH_d^* and ΔS_d^* values of $LnK21DA^+$ and $LnK22DA^+$ complexes, it is observed that the activation entropy barrier is the dominant factor in controlling the direct dissociation of $LnK21DA^+$ and $LnK22DA^+$ complexes, *i.e.* entropy-controlled solvolytic dissociation kinetics,[26] but it is relatively less important in the acetate-dependent dissociation of $LnDO2A^+$ complexes, particularly for the heavy $LnDO2A^+$ complexes. On the other hand, activation enthalpy barrier is the dominant factor in controlling the proton-dependent, limiting-rate dissociation pathway for heavy $LnK21DA^+$ and $LnDO2A^+$ complexes (*vide infra*).

$LnDO2A^+$ dissociation reactions in the pH range 1.75–2.65

An indicator method similar to the one used to study metal ion–DOTA complex formation was chosen to study $LnDO2A^+$ dissociation reactions (eqn (11)) in the pH range 1.75–2.65.[27]

$$LnDO2A^+ + nH^+ \rightarrow Ln^{3+} + H_nDO2A^{(n-2)+},\ n = 1\text{–}4 \qquad (11)$$

In this case, the pre-formed complex is subjected into an acid solution with a dye indicator, cresol red. The cresol red has strong absorption in the UV-Vis range and the changes of absorbance values at 247 and 518 nm vary with $[H^+]$, in a linear relationship. As the complex dissociates, the ligand is protonated and causes slight incremental increases in solution pH which can be shown by the indicator absorbance changes, and the rate could be monitored. The experimental rate data of the $LnDO2A^+$ dissociation reaction monitored by the indicator method fit pseudo-first-order kinetics. However, because the absorbance change is usually small, this method could cause relatively larger uncertainties with still acceptable results for the determination of the dissociation rates.

Dissociation kinetics. When $LnDO2A^+$ dissociates, two equivalents of protons would need to occupy the DO2A nitrogen protonation sites with pK_a values 10.94 and 9.55, respectively. The third and fourth DO2A protonation sites are at the carboxylate positions with the respective pK_a values 3.85 and 2.55. At the present $[H^+]$ range studied, *i.e.* 0.00288–0.0346 mol dm^{-3}, the third protonation site will also be occupied. The minimum concentration of the strong acid ($HClO_4$) required to induce ≥99% dissociation of $LnDO2A^+$ is $3 \times 5.0 \times 10^{-4}$ mol dm^{-3} $= 1.5 \times 10^{-3}$ mol dm^{-3} which is about 48% less than the lowest $HClO_4$ concentration (0.00288 mol dm^{-3}) employed for the current study. Thus, the pseudo-first order condition required for $[H^+]$ is no longer maintained. In cases like this, the initial rate method was used to obtain the k_{obs} values. Table S4 (ESI†) lists the k_{obs} values and plots of these values *vs.* $[H^+]$ at the four temperatures studied display a first-order dependence, without the saturation behavior, *e.g.* Fig. 4.

A general reaction scheme consistent with the observed behavior for these complexes is given below (Scheme 3), where Ln, L, LnL and LnHL are the Ln(III) ion, ligand (DO2A), Ln(III) complex and protonated Ln(III) complex, respectively.

$$Ln^{3+} + HnL \underset{}{\overset{kd}{\longleftarrow}} LnL^+ + H^+ \xrightarrow{k_H} \left[LnLH^{2+}\right] \xrightarrow[fast]{H^+} Ln^{3+} + HnL$$

Scheme 3 The proposed mechanisms for the dissociation of $LnDO2A^+$ in the pH range 1.75–2.65.

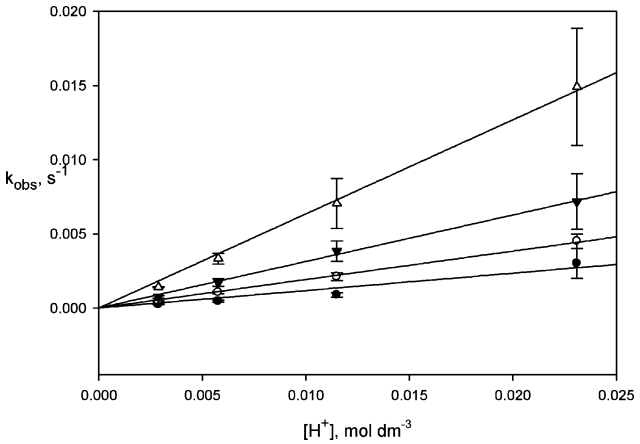

Fig. 4 Plots of the dissociation k_{obs} values *vs.* $[H^+]$ for the $EuDO2A^+$ complex at different temperatures: 19 °C (●); 25 °C (○); 33 °C (▼); 41 °C (△).

The observed rate constants for the Ln(III) complexes obey the rate law:

$$k_{obs} = k_d + k_H[H^+] \qquad (12)$$

where k_d and k_H are the respective direct and proton-catalyzed dissociation rate constants. Fitting the k_{obs} data to eqn (12) gives the intercept values k_d and the slope values k_H. However, due to the relatively greater uncertainties of rate constant measurements particularly at lower $[H^+]$ discussed above, the fits of k_d values were scattered around zero and the direct dissociation pathways were assumed to be not significant. The k_{obs} data were therefore fitted to the simplified eqn ($k_{obs} = k_H[H^+]$ and the results are listed in Table 4. Similar results were reported for rates of dissociation of complexes formed with other macrocyclic ligands.[28]

The proton-catalyzed $LnDO2A^+$ dissociation pathways go through monoprotonated adducts. It is possible that the initial proton attack occurs at a dissociated carboxylate oxygen. The protonated species then dissociate directly. The rate-determining step is probably associated with the distortion of the macrocycle ring and/or the protonation of the first nitrogen site. At a given temperature, both the k_{obs} and the resolved k_H values decrease in the order: $LaDO2A^+ > PrDO2A^+ > ErDO2A^+ > EuDO2A^+ > LuDO2A^+$. This is roughly consistent with the fact that $LnDO2A^+$ complex formation stability increases with increasing atomic number (except that of Er and Eu), indicating that ionic interaction between the Ln(III) ion and the macrocyclic ligand is probably the major one. The absence of k_d values indicates that these complexes

Table 4 The k_H values for the dissociation reactions of $LnDO2A^+$ at 19, 25, 33 and 41 °C

	k_H/mol^{-1} dm^3 s^{-1}				
T/°C	La	Pr	Eu	Er	Lu
19		$(2.36 \pm 0.05) \times 10^{-1}$	$(1.17 \pm 0.13) \times 10^{-1}$	$(1.21 \pm 0.17) \times 10^{-1}$	$(1.59 \pm 0.12) \times 10^{-2}$
25	2.23 ± 0.13	$(3.66 \pm 0.06) \times 10^{-1}$	$(1.92 \pm 0.04) \times 10^{-1}$	$(2.49 \pm 0.22) \times 10^{-1}$	$(2.34 \pm 0.23) \times 10^{-2}$
33		$(8.65 \pm 1.08) \times 10^{-1}$	$(3.14 \pm 0.07) \times 10^{-1}$	$(5.75 \pm 0.06) \times 10^{-1}$	$(8.54 \pm 0.30) \times 10^{-2}$
41		1.00 ± 0.03	$(6.34 \pm 0.14) \times 10^{-1}$	1.15 ± 0.06	$(1.57 \pm 0.04) \times 10^{-1}$

Table 5 Activation parameters for proton-catalyzed dissociation of selected $LnDO2A^+$, $LnK21DA^+$ and $LnK22DA^+$ complexes in the pH range 1.75–2.65; ΔG_H^* values are calculated at 25 °C[a]

	$LnDO2A^+$			$LnK21DA^+$			$LnK22DA^+$		
	ΔH_H^*/kcal	ΔS_H^*/cal K^{-1}	ΔG_H^*/kcal	ΔH_H^*/kcal	ΔS_H^*/cal K^{-1}	ΔG_H^*/kcal	ΔH_H^*/kcal	ΔS_H^*/cal K^{-1}	ΔG_H^*/kcal
La	n/a			6.5	−23.7	13.6	12.9	−17.4	18.1
Pr	12.2 ± 2.3	−19.5 ± 7.5	18.0	n/a			n/a		
Eu	13.1 ± 0.8	−18.0 ± 2.6	18.4	7.4	−26.9	15.4	6.5	−37.7	17.7
Er	18.1 ± 0.6	−0.92 ± 2.2	18.3	n/a			n/a		
Lu	19.6 ± 2.4	0.25 ± 7.9	19.5	n/a			7.7	−31.7	17.2

[a] $[H^+] = 2.88 \times 10^{-3}$–$2.31 \times 10^{-2}$ mol dm^{-3} for LnDO2A; $[H^+] = 8.4 \times 10^{-6}$–$2.47 \times 10^{-4}$ mol dm^{-3} for LnK21DA; $[H^+] = 5 \times 10^{-4}$–7.5×10^{-3} mol dm^{-3} for LnK22DA.

are structurally rigid, probably due to that the ligand DO2A is pre-organized. This is true for other cyclen-structurally related lanthanide complexes such as $LnDO3A$[2c] and $LnDOTA^-$.[2d]

Activation parameters. The activation parameters for the proton-dependent pathways have been obtained from the Eyring plots using the temperature-dependent rate constants and are listed in Table 5 (plots not shown), together with those of $LnK21DA^+$ and $LnK22DA^+$ complexes for comparison purposes. The ΔG_H^* values of the $LnDO2A^+$ complexes are, as expected, smaller than both ΔG_{AC}^* and ΔG_{lim}^* values obtained at higher pH range. On the other hand, these ΔG_H^* values are larger than those of the corresponding $LnK21DA^+$ and $LnK22DA^+$ complexes, reflecting the greater thermodynamic stability and kinetic inertness of the $LnDO2A^+$ complexes. The isokinetic (linear) relationship observed for the higher pH range is also observed in this lower pH range when the values of ΔH^* are plotted against those of ΔS^* (Fig. 3).

In general, the dissociation has higher activation ΔH_H^* enthalpy barrier for the $LnDO2A^+$ complexes than those of $LnK21DA^+$ and $LnK22DA^+$ complexes, except possibly $LaDO2A^+$. Among the $LnDO2A^+$ complexes studied, heavier $LnDO2A^+$ complexes tend to have greater ΔH_H^* barriers than those of the lighter complexes. On the other hand, the activation entropy barriers become the controlling factor for the dissociation of the $LnK21DA^+$ and $LnK22DA^+$ complexes, except for $LaK21DA^+$. The relative activation entropy barrier toward ΔG_H^* is in the order $LnDO2A^+$ < $LnK21DA^+$ < $LnK22DA^+$. One possible way to explain these observations is to consider the ligand cavity size-Ln(III) ion diameter fit, the strength of ionic interaction between the ligand and the Ln(III) ion, and the overall formation stability of the Ln(III) macrocyclic complex. Fig. 5 shows the plots of the log K_f values for the Ln(III) complexes of DO2A,[4f] K21DA[1c] and K22DA.[1a] It is seen that DO2A with the smallest 12-membered macrocyclic cavity size among the three ligands tends to form stronger complexes with heavier Ln(III) ions due to mainly strong ionic interactions. However, the fact that the stabilities for the $LnDO2A^+$ complexes from Sm(III) to Lu(III) do not very as much as those from La(III) to Nd(III) indicate probably that the negative cavity size effect tends to be gradually important in going from the smaller, heavier Ln(III) ions to the larger, lighter Ln(III) ions. On the other hand, K22DA with a 18-membered macrocyclic ring forms stronger complexes with the larger, lighter Ln(III) ions due to its better cavity size to Ln(III) ion diameter fit, allowing perhaps close-to-normal Ln(III) ion–ligand ionic interactions without too much ligand stereochemical constraints (*i.e.* structural "dislocation").[29] The stability trend of the $LnK21DA^+$ complexes with 15-membered macrocycles could be considered as the compromise of that discussed above for the $LnDO2A^+$ and $LnK22DA^+$ complexes.

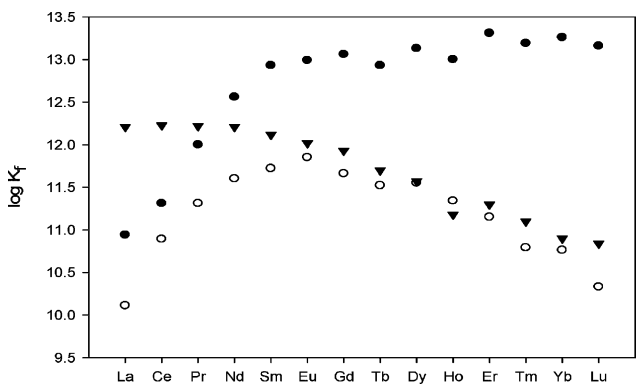

Fig. 5 Plots of the log K_f values for the Ln(III) complexes of DO2A (●, ref. 4*f*), K21DA (○, ref. 1*c*) and K22DA (▼, ref. 1*a*).

The following two simple postulates are tentatively proposed to account for the general activation parameter observations for the Ln(III) macrocyclic complexes discussed above:

1. Complexes with greater formation stabilities tend to have greater ΔH_H^* barriers relative to others of the same macrocyclic ligand.

2. The more macrocyclic ligand conformational flexibility, the greater the relative ΔS_H^* barrier toward ΔG_H^*.

It is known that the formation of Ln(III)-18-crown-6 complexes are entropy driven.[30] Formation of Ln(III) complexes with N-donor ligands is also entropy-driven but has high activation enthalpies.[31] It was also reported that the activation parameters for the formation and dissociation reactions of dioxouranium(VI)–diphosphonic acid complexes are comparable, and although the kinetic activation enthalpy barriers are greater, the thermodynamic stabilities are driven by favorable entropy change.[32] Note that there are still subtle variations remained to be explained to test the above postulates, *e.g.* why the activation enthalpy barrier of $LuK22DA^+$ is greater that of $EuK22DA^+$.

Comparisons of the dissociation kinetic data of $LnDO2A^+$ with other Ln(III) macrocyclic complexes

$LnDO2A^+$ (LnL^+) complexes are suitable candidates for the study of dissociation kinetics in a wide pH range; the fast equilibrium formation of the metastable intermediate ($LnLH^{2+}$) at higher pH is

Table 6 Various kinetic rate and equilibrium constants of selected macrocyclic Ln(III) complexes at 25 °C

Ln complex	k_d/s^{-1}	k_H/mol^{-1} dm^3 s^{-1}	k_{lim}/s^{-1}	K'/mol^{-1} dm^3
LaDO2A$^{+,a}$	$(3.09 \pm 0.79) \times 10^{-4}$	2.23 ± 0.13	$(2.70 \pm 0.53) \times 10^{-3}$	$(4.91 \pm 2.20) \times 10^{+3}$
PrDO2A$^{+,a}$	$(1.94 \pm 0.40) \times 10^{-5}$	$(3.66 \pm 0.06) \times 10^{-1}$	$(2.29 \pm 0.11) \times 10^{-4}$	$(8.06 \pm 1.30) \times 10^{+3}$
EuDO2A$^{+,a}$	$(7.83 \pm 2.68) \times 10^{-6}$	$(1.92 \pm 0.04) \times 10^{-1}$	$(1.14 \pm 0.15) \times 10^{-4}$	$(5.48 \pm 1.76) \times 10^{+3}$
ErDO2A$^{+,a}$	$(3.05 \pm 0.94) \times 10^{-6}$	$(2.49 \pm 0.22) \times 10^{-1}$	$(1.80 \pm 0.46) \times 10^{-4}$	$(1.58 \pm 0.56) \times 10^{+3}$
LuDO2A$^{+,a}$	$(4.99 \pm 1.34) \times 10^{-7}$	$(2.34 \pm 0.23) \times 10^{-2}$	$(3.20 \pm 0.33) \times 10^{-5}$	$(2.31 \pm 0.38) \times 10^{+3}$
CeDO3A^b		$(1.8 \pm 0.8) \times 10^{-3}$		
GdDO3A^b		$(4.4 \pm 0.1) \times 10^{-4}$		
GdDOTA$^{-,c}$		$\sim 10^{-7}$–5×10^{-10}		
CeTETA$^{-,d}$	0.101	56.7		
LaK21DA$^{+,e}$	$(4.69 \pm 0.15) \times 10^{-2}$	$(7.18 \pm 0.11) \times 10^{2}$		
PrK21DA$^{+,e}$	$(4.14 \pm 0.20) \times 10^{-3}$	$(8.19 \pm 0.15) \times 10^{1}$		
EuK21DA$^{+,e}$	$(1.76 \pm 0.06) \times 10^{-3}$	$(3.11 \pm 0.04) \times 10^{1}$		
ErK21DA$^{+,e}$	$(3.32 \pm 0.13) \times 10^{-3}$		$(1.04 \pm 0.12) \times 10^{-2}$	$(6.64 \pm 0.85) \times 10^{+3}$
LuK21DA$^{+,e}$	$(1.08 \pm 0.06) \times 10^{-2}$		$(4.11 \pm 0.36) \times 10^{-2}$	$(1.22 \pm 0.11) \times 10^{+4}$
LaK22DA$^{+,f}$	$(3.97 \pm 0.20) \times 10^{-4}$	1.21 ± 0.02		
PrK22DA$^{+,f}$	$(9.14 \pm 1.40) \times 10^{-5}$	$(5.36 \pm 0.09) \times 10^{-1}$		
EuK22DA$^{+,f}$	$(4.31 \pm 1.47) \times 10^{-4}$	$(5.70 \pm 0.96) \times 10^{-1}$		
LuK22DA$^{+,f}$	$(5.58 \pm 0.87) \times 10^{-4}$	1.64 ± 0.08		
EuAc$_3$[15]N$_3$O$_2$^{g}	$(1.62 \pm 0.03) \times 10^{-5}$	1.38 ± 0.06		
EuAc$_3$[18]N$_3$O$_3$^{h}	$(1.32 \pm 0.03) \times 10^{-1}$	$(9.76 \pm 0.12) \times 10^{3}$		

^{a} This work; $k_d = k_{AC}$[Acetate = 0.005 mol dm^{-3}]. ^{b} Ref. 2*c*. ^{c} Ref. 10*b*, 28. ^{d} Ref. 2*d*. ^{e} Ref. 2*a*. ^{f} Ref. 2*b*. ^{g} Ref. 18. ^{h} Ref. 19.

no longer stable at lower pH and the proton-dependent saturation behavior at higher pH becomes linear dependent at lower pH. The kinetic data obtained for the LnDO2A$^+$ complexes in two pH ranges allow their comparisons with the more stable cyclen-based complexes (*e.g.* LnDOTA$^-$ and LnDO3A) and complexes with larger macrocyclic rings (*e.g.* LnK22DA$^+$ > LnK21DA$^+$).

The formation stability constants for a number of cyclen-based macrocyclic Ln(III) complexes are in the order LnDOTA$^-$ > LnDO3A > LnDO2A$^+$. For macrocyclic ligands with 12, 15 and 18-membered rings respectively, the order is LnDO2A$^+$ > LnK22DA$^+$ > LnK21DA$^+$, with a few exceptions (*e.g.* LnDO2A$^+$ where Ln = La, Ce and Pr). The larger macrocycles, K22DA and K21DA are more flexible than the smaller 12-membered ring DO2A. The basicity of DO2A is also greater than K21DA and K22DA.

Table 6 lists various kinetic rate and equilibrium constants of selected macrocyclic lanthanide complexes at 25 °C. The overall dissociation rate constant k_H should be in the following order and are found as expected: LnDOTA$^-$ < LnDO3A < LnDO2A$^+$ < LnK22DA$^+$ < LnK21DA$^+$. For example, for GdDOTA$^-$, GdDO3A, EuDO2A$^+$, EuK22DA$^+$, EuK21DA$^+$ complexes at 25 °C, the measured k_H values are: ~0 (not observed), 4.4×10^{-4}, 1.92×10^{-1}, 0.57 and 31.1, respectively. (The data of Gd(III) complexes are used when Eu(III) data were not available).

The complexes CeTETA$^-$ ($\log K_f$ = 13.12, TETA is 1,4,8,11-tetraazacyclotetradecane-1,4,8,11-tetraacetic acid)[4d] and EuAc$_3$[18]N$_3$O$_3$ ($\log K_f$ = 17.26, Ac$_3$[18]N$_3$O$_3$ is 1,7,13-trioxa-4,10,16-triazacyclooctadecane-*N*,*N*′*N*″-triacetic acid)[21] have much faster dissociation kinetic rates as compared to their structural analogues with similar complex formation stabilities. This is presumably because both ligands are either not pre-organized for metal ion complexation[2e] or have a number of isomeric structures with much more flexible ring conformations,[21] which lead to faster dissociation rates.

Concerning the formation constants of LnDO2A$^+$ and summary

In a previous paper we have used an extra-thermodynamic relationship of a good linear correlation between the $\log K_{CaL}$ values and $\log K_{GdL}$ values (r^2 = 0.95) for a number of selected macrocyclic and linear aminopolycarboxylate ligands to estimate that the $\log K_{GdDO2A^+}$ value should be in the range 12–13, and is consistent with what we obtained.[4f] From the present kinetic studies, we found that the k_H values for the LnDO2A$^+$ complexes ($\log K$ range = 10.94–13.16) are closer to those of the LnK22DA$^+$ complexes ($\log K$ range = 12.21–10.84). For example, the LaDO2A$^+$ complex with a $\log K$ value of 10.94 has a k_H value of 2.23 mol^{-1} dm^3 s^{-1}, which is greater than that of the LaK22DA$^+$ complex (1.21 mol^{-1} dm^3 s^{-1}) and is consistent with a higher $\log K$ value of 12.21 for the LaK22DA$^+$ complex. Similarly, EuDO2A$^+$ ($\log K$ = 12.99) has a k_H value of 0.192 mol^{-1} dm^3 s^{-1} and is smaller than that of EuK22DA$^+$ (k_H = 0.570 mol^{-1} dm^3 s^{-1}, $\log K$ 12.02).

In summary, LnDO2A$^+$ (LnL$^+$) complexes are suitable candidates for the study of dissociation kinetics in a wide pH range; the metastable intermediate (LnLH^{2+}) at higher pH is no longer stable at lower pH and the acid-dependent saturation behavior at higher pH becomes linear dependence at lower pH. The absence of an [H$^+$]-independent pathway in both pH ranges indicates that LnDO2A$^+$ complexes are kinetically rather inert. The obtained k_{AC} values follow the order: LaDO2A$^+$ > PrDO2A$^+$ > EuDO2A$^+$ > ErDO2A$^+$ > LuDO2A$^+$, whereas the k_{lim} and k_H values follow the order: LaDO2A$^+$ > PrDO2A$^+$ > ErDO2A$^+$ > EuDO2A$^+$ >

LuDO2A$^+$, mostly consistent with their thermodynamic stability order, *i.e.* the more thermodynamically stable the more kinetically inert. Of some interest is that acetate catalysis constitutes an unprecedented 87% of the dissociation pathway of the LaDO2A$^+$ complex at [Acetate] = 5.0 mmol dm^{-3}, 25 °C.

Experimental

Materials and standard solutions

Reagent grade lithium acetate (Aldrich), lithium perchlorate (Aldrich), lanthanide (La, Ce, Pr, Eu, Er, Lu) nitrates (Aldrich/Alfa), copper nitrate (MCB), acetic acid (MCB), perchloric acid (Fisher) and other reagents were used as received. The ligand DO2A was synthesized by following a procedure published elsewhere[9c] and was found to be analytically and spectroscopically pure. All solutions were made in deionized water. Aqueous solutions of the ligand were prepared by weight and standardized by potentiometric and complexometric titrations with standardized NaOH solution and cerium nitrate solutions, respectively.[1a,c] Standard solutions (~0.01 mol dm^{-3}) of lanthanide nitrates were standardized by EDTA titrations with xylenol orange as indicator.

Complexes were made in situ by mixing appropriate amounts of lanthanide nitrate and ligand solutions (molar ratio ~ 1.02 : 1.0) and adjusting the pH to *ca.* 6.5–7.0 with $(CH_3)_4NOH$. For studies at high pH range, the complex concentration in the reaction mixtures was kept at 5.0×10^{-5} mol dm^{-3} and the buffer solutions were made by using a constant acetate ion concentration (*e.g.* 5×10^{-3} mol dm^{-3}) and varying [Acetic acid]. For studies at lower pH, the pH of each solution was adjusted by $HClO_4$ and the final concentration of reagents were [LnDO2A$^+$] = 5.0×10^{-4} mol dm^{-3}, [cresol red] = 4.17×10^{-5} mol dm^{-3}. The ionic strength was adjusted to 0.1 mol dm^{-3} with $LiClO_4$ for studies at both pH ranges. Hydrogen ion concentrations were calculated from the pH measurements by the expression $-\log[H^+] = pH - 0.11$.[2a]

Kinetic measurements

Spectra and kinetic runs were made with a Hewlett Packard 8453 diode-array spectrophotometer equipped with a thermostat cell holder with a constant temperature circulating bath (FIRSTEK SCIENTIFIC B403). The solution temperature was controlled to within ±0.1 °C. For studies at higher pH range, as the Ln(III) complexes do not show appreciable absorption in the near-ultraviolet region, copper(II) ion (1.0×10^{-3} mol dm^{-3}, 20 fold) was used as the scavenger of the free ligand and the reaction kinetics were followed by monitoring the growth in absorbance due to the CuDO2A complex formation at 280 nm. For studies at lower pH, the dye, cresol red, was used to monitor the dissociation rate due to the fact that complex dissociation results in slight pH increase and therefore the cresol red absorbance changes.[27] The absorbance changes of cresol red at 247 and 518 nm in the range of 0.02–0.1 unit were measured.

In most cases, pseudo-first order rate constants (k_{obs}) were calculated using the integral rate method by fitting the absorbance (A) *vs.* time (t) data for at least three half-lives to the equation: $A_t = A_0 + A_\infty(1 - e^{-k_{obs}t})$, where A_t, A_o and A_∞ are the instantaneous, initial and final absorbance values, respectively. In a few cases, particularly in the lower pH range studies involving low [H$^+$] and the faster dissociating LaDO2A$^+$ complex, the initial rate method was employed to obtain the k_{obs} values by fitting the data to the equation: $\Delta A/\Delta t/(b\varepsilon_\lambda) = k_{obs}[ML]_0$, where ΔA is the change of absorbance in the time period Δt, b = 1.0, ε_λ is the molar absorptivity of cresol red at the wavelength λ, and $[ML]_0$ is the initial LnDO2A$^+$ concentration. Sigma plots were used for curve fitting. Each value of k_{obs} reported represents the average of three replicate runs.

Acknowledgements

The authors wish to thank the National Science Council of the Republic of China (Taiwan) for financial support (grant number NSC-98-2113-M-010-001-MY3).

References

1 (*a*) C. A. Chang and M. E. Rowland, *Inorg. Chem.*, 1983, **22**, 3866–3869; (*b*) C. A. Chang, V. O. Ochaya and V. C. Sekhar, *J. Chem. Soc., Chem. Commun.*, 1985, 1724–1725; (*c*) C. A. Chang and V. O. Ochaya, *Inorg. Chem.*, 1986, **25**, 355–358; (*d*) C. A. Chang, P. H. L. Chang and S. Qin, *Inorg. Chem.*, 1988, **27**, 944–946; (*e*) J. F. Carvalho, S.-H. Kim and C. A. Chang, *Inorg. Chem.*, 1992, **31**, 4065–4068.

2 (*a*) V. C. Sekhar and C. A. Chang, *Inorg. Chem.*, 1986, **25**, 2061–2065; (*b*) C. A. Chang and V. C. Sekhar, *Inorg. Chem.*, 1987, **26**, 1981–1985; (*c*) K. Kumar, C. A. Chang and M. F. Tweedle, *Inorg. Chem.*, 1993, **32**, 587–593; (*d*) C. A. Chang and Y.-L. Liu, *J. Chin. Chem. Soc.*, 2000, **47**, 1001–1006; (*e*) C. A. Chang, Y.-L. Liu, C.-Y. Chen and X.-M. Chou, *Inorg. Chem.*, 2001, **40**, 3448–3455.

3 (*a*) K. Kumar, C. A. Chang, L. C. Francesconi, M. F. Malley, K. Kumar, J. Z. Gougoutas, M. F. Tweedle, D. W. Lee and L. J. Wilson, *Inorg. Chem.*, 1993, **32**, 3501–3508; (*b*) C. A. Chang, L. Francesconi, D. Dischino, M. Malley, J. Z. Gougoutas and M. F. Tweedle, *Inorg. Chem.*, 1994, **33**, 3567–3575; (*c*) K. Kumar, M. F. Tweedle, M. F. Malley and J. Z. Gougoutas, *Inorg. Chem.*, 1995, **34**, 6472–6480.

4 (*a*) R. C. Holz, S. L. Klakamp, C. A. Chang, W. Dew and Horrocks Jr., *Inorg. Chem.*, 1990, **29**, 2651–2658; (*b*) C. A. Chang, H. G. Brittain, J. Telser and M. F. Tweedle, *Inorg. Chem.*, 1990, **29**, 4468–4473; (*c*) R. C. Holz, S. L. Klakamp, C. A. Chang, W. Dew and Horrocks Jr., *Inorg. Chem.*, 1991, **30**, 3270–3275; (*d*) X. Zhang, C. A. Chang, H. G. Brittain, J. M. Garrison, J. Telser and M. F. Tweedle, *Inorg. Chem.*, 1992, **31**, 5597–5600; (*e*) S. Frey, C. A. Chang, W. Dew and Horrocks Jr., *Inorg. Chem.*, 1994, **33**, 2882–2889; (*f*) C. A. Chang, F. K. Shieh, Y.-L. Liu, Y.-H. Chen, H.-Y. Chen and C.-Y. Chen, *J. Chem. Soc., Dalton Trans.*, 1998, 3243–3248.

5 (*a*) P. Caravan, J. J. Ellison, T. J. McMurry and R. B. Lauffer, *Chem. Rev.*, 1999, **99**, 2293–2352; (*b*) C. A. Chang, *Eur. J. Solid State Inorg. Chem.*, 1991, **28**, 237–244; (*c*) C. A. Chang, P. F. Sieving, A. D. Watson, T. M. Dewey, T. B. Karpishin and K. N. Raymond, *J. Magn. Reson. Imaging*, 1992, **2**, 95–98; (*d*) C. A. Chang, *Invest. Radiol.*, 1993, **28**, S21–27; (*e*) J. Varadarajan, S. Crofts, J. D. Fellmann, J. C. Carvalho, S. Kim, C. A. Chang and A. Watson, *Invest. Radiol.*, 1994, **29**, S18–S20; (*f*) T.-Z. Lee, T.-H. Cheng, M.-H. Ou, C. A. Chang, G. C. Liu and Y.-M. Wang, *Magn. Reson. Chem.*, 2004, **42**, 329–336; (*g*) V. Jacques and J. F. Desreux, *Top. Curr. Chem.*, 2002, **221**, 123–164; (*h*) P. Hermann, J. Kotek, V. Kubicek and I. Lukes, *Dalton Trans.*, 2008, 3027–3047; (*i*) *Medicines and Healthcare Products Regulatory Agency. Drug Safety Update*, August 2007, pp. 2–4; (*j*) A. Kribben, O. Witzke, U. Hillen, J. Barkhausen, A. E. Daul and R. Erbel, *J. Am. Coll. Cardiol.*, 2009, **53**, 1621–1628.

6 S. Liu and D. S. Edwards, *Bioconjugate Chem.*, 2001, **12**, 7–34.

7 C. M. G. dos Santos, A. J. Harte, S. J. Quinn and T. Gunnlaugsson, *Coord. Chem. Rev.*, 2008, **252**, 2512–2527.

8 (*a*) V. K. Manchanda and C. A. Chang, *Anal. Chem.*, 1986, **58**, 2269–2275; (*b*) V. K. Manchanda and C. A. Chang, *Anal. Chem.*, 1987, **59**, 813–818; (*c*) C. A. Chang, V. K. Manchanda and J. Peng, *Inorg. Chim.*

Acta, 1987, **130**, 117–118; (*d*) V. K. Manchanda, C. A. Chang and J. Peng, *Solvent Extr. Ion Exch.*, 1988, **6**, 835–857; (*e*) C. A. Chang, V. K. Manchanda and J. Peng, *Solvent Extr. Ion Exch.*, 1989, **7**, 413–433.
9 (*a*) C. A. Chang, B.-H. Wu and P.-Y. Kuan, *Inorg. Chem.*, 2005, **44**, 6646–6654; (*b*) C. A. Chang, Y.-P. Chen and C.-H. Hsiao, *Eur. J. Inorg. Chem.*, 2009, 1036–1042; (*c*) C. A. Chang, C.-H. Hsiao and B.-H. Wu, *Eur. J. Inorg. Chem.*, 2009, 1339–1346.
10 (*a*) E. Brucher and A. D. Sherry, *Inorg. Chem.*, 1990, **29**, 1555–1559; (*b*) E. Toth, E. Brucher, I. Lazar and I. Toth, *Inorg. Chem.*, 1994, **33**, 4070–4076; (*c*) K. Kumar, C. A. Chang and M. F. Tweedle, *Inorg. Chem.*, 1993, **32**, 587–593; (*d*) K. Y. Choi, J. C. Kim and D. W. Kim, *J. Coord. Chem.*, 1993, **30**, 1; (*e*) K. Y. Choi, K. S. Kim and J. C. Kim, *Bull. Chem. Soc. Jpn.*, 1994, **67**, 267; (*f*) K. Y. Choi, K. S. Kim and J. C. Kim, *Polyhedron*, 1994, **13**, 567; (*g*) K. Y. Choi, D. W. Kim and C. P. Hong, *Polyhedron*, 1995, **14**, 1299.
11 (*a*) J. Huskens, D. A. Torres, Z. Kovacs, J. P. Andre, C. F. C. Geraldes and A. D. Sherry, *Inorg. Chem.*, 1997, **36**, 1495–1503; (*b*) W. D. Kim, D. C. Hrncir, G. E. Kiefer and A. D. Sherry, *Inorg. Chem.*, 1995, **34**, 2225–2232.
12 C. A. Chang, C. Y. Chen and H. Y. Chen, *J. Chin. Chem. Soc.*, 1999, **46**, 519–529.
13 J. W. Weeks, M. R. Taylor and K. P. Wainwright, *J. Chem. Soc., Dalton Trans.*, 1997, 317–322.
14 T. M. Jones-Wilson, K. A. Deal, C. J. Anderson, D. W. McCarthy, Z. Kovas, R. J. Motekaitis, A. D. Sherry, A. E. Martell and M. J. Welch, *Nucl. Med. Biol.*, 1998, **25**, 523–530.
15 G. A. Nyssen and D. W. Margerum, *Inorg. Chem.*, 1970, **9**, 1814.
16 M. De Jonghe and W. D'olieslager, *Inorg. Chim. Acta*, 1985, **109**, 7.
17 E. Balogh, R. Tripier, R. Ruloff and E. Toth, *Dalton Trans.*, 2005, 1058–1065.
18 K.-Y. Choi, D. W. Kim and C. P. Hong, *Polyhedron*, 1995, **14**, 1299–1306.
19 K.-Y. Choi, D. W. Kim, C. S. Kim, C. P. Hong, H. Ryu and Y.-I. Lee, *Talanta*, 1997, **44**, 527–534.
20 R. Delgado, Y. Sun, R. J. Motekaitis and A. E. Martell, *Inorg. Chem.*, 1993, **32**, 3320–3326.
21 Y. Wang, W. Dew and Horrocks Jr., *Inorg. Chim. Acta*, 1997, **263**, 309–314.
22 D. Chen, P. J. Squattrito and A. E. Martell, *Inorg. Chem.*, 1990, **29**, 4366–4368.
23 J. H. Espenson, *Chemical Kinetics and Reaction Mechanisms*, McGraw-Hill Book Co., New York, 1981.
24 (*a*) R. G. Wilkins, *Kinetics and Mechanism of Reactions of Transition Metal Complexes*, 2nd edn, VCH Weinheim, Germany, 1991. pp. 108–109; (*b*) R. G. Wilkins, *Kinetics and Mechanism of Reactions of Transition Metal Complexes*, 2nd edn, VCH Weinheim, Germany, 1991. pp. 105–106.
25 A. Ekstrom, L. F. Lindoy and R. D. Smith, *Inorg. Chem.*, 1980, **19**, 724–727.
26 S. Saito, H. Hoshino and T. Yotsuyanagi, *Inorg. Chem.*, 2001, **40**, 3819–3823.
27 S. P. Kasprzyk and R. G. Wilkins, *Inorg. Chem.*, 1982, **21**, 3349–3352.
28 G. Tircso, Z. Kovacs and A. D. Sherry, *Inorg. Chem.*, 2006, **45**, 9269–9280.
29 L. F. Lindoy, *Pure Appl. Chem.*, 1997, **69**, 2179–2186.
30 R. M. Izatt, J. D. Lamb and J. J. Christensen, *J. Am. Chem. Soc.*, 1977, **99**, 8344–8346.
31 V. Hubscher-Bruder, J. Haddaoui, S. Bouhroum and F. Arnaud-Neu, *Inorg. Chem.*, 2010, **49**, 1363–1371.
32 M. A. Hines, J. C. Sullivan and K. L. Nash, *Inorg. Chem.*, 1993, **32**, 1820–1823.